Title

The TSC1-mTOR-PLK axis regulates the homeostatic switch from Schwann cell proliferation to myelination in a stage-specific manner

Journal

Glia, 66(9)

ISSN

0894-1491

Authors

Jiang, Minqing
Rao, Rohit
Wang, Jincheng
et al.

Publication Date

2018-09-01

DOI

10.1002/glia.23449

Peer reviewed

HHS Public Access

Author manuscript

Glia. Author manuscript; available in PMC 2019 September 01.

Published in final edited form as:

Glia. 2018 September ; 66(9): 1947–1959. doi:10.1002/glia.23449.

The TSC1-mTOR-PLK Axis Regulates the Homeostatic Switch from Schwann Cell Proliferation to Myelination in a Stage-specific Manner

Minqing Jiang[1,2,*], **Rohit Rao**[1,*], **Jincheng Wang**[1], **Jiajia Wang**[1], **Lingli Xu**[1], **Lai Man Wu**[1], **Jonah R. Chan**[3], **Huimin Wang**[2], and **Q. Richard Lu**[1,#]

[1]Department of Pediatrics, Division of Experimental Hematology and Cancer Biology, Cincinnati Children's Hospital Medical Center, University of Cincinnati, Cincinnati, Ohio, USA

[2]The Institute of Cognitive Neuroscience, East China Normal University, Shanghai, China

[3]Department of Neurology and Programs in Biomedical and Neurosciences, University of California, San Francisco, CA 94158

Abstract

Proper peripheral myelination depends upon the balance between Schwann cell proliferation and differentiation programs. The serine/threonine kinase mTOR integrates various environmental cues to serve as a central regulator of cell growth, metabolism, and function. We report here that tuberous sclerosis complex 1 (TSC1), a negative regulator of mTOR activity, establishes a stage-dependent program for Schwann cell lineage progression and myelination by controlling cell proliferation and myelin homeostasis. *Tsc1* ablation in Schwann cell progenitors in mice resulted in activation of mTOR signaling, and caused over-proliferation of Schwann cells and blocked their differentiation, leading to hypomyelination. Transcriptome profiling analysis revealed that mTOR activation in *Tsc1* mutants resulted in upregulation of a polo-like kinase (PLK)-dependent pathway and cell cycle regulators. Attenuation of mTOR or pharmacological inhibition of polo-like kinases partially rescued hypomyelination caused by *Tsc1* loss in the developing peripheral nerves. In contrast, deletion of *Tsc1* in mature Schwann cells led to redundant and overgrown myelin sheaths in adult mice. Together, our findings indicate stage-specific functions for the TSC1-mTOR-PLK signaling axis in controlling the transition from proliferation to differentiation and myelin homeostasis during Schwann cell development.

Graphical Abstract

Correspondence: Dr. Q. Richard Lu, Cincinnati Children's Hospital Medical Center, University of Cincinnati, Cincinnati, OH 45229, USA; richard.lu@cchmc.org. Tel: 513-636-7684; Fax: 513-803-0783.

*These authors contributed equally

Conflict of Interest: The authors declare no competing financial interests.

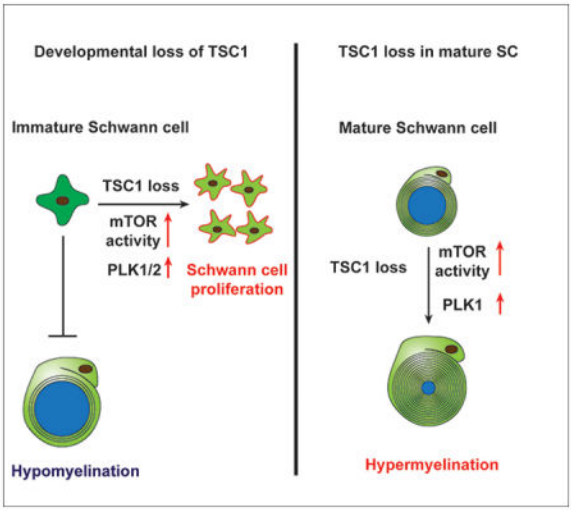

Keywords

Tumor Suppressor; TSC; mTOR signaling; Polo-like Kinase; Schwann Cell; Proliferation; myelination

Introduction

Myelination of axons is vital for rapid saltatory conduction of action potentials and effective sensorimotor integration. In the peripheral nervous system (PNS), Schwann cells (SCs) wrap large-caliber axons to form tightly compacted myelin sheaths. Defects in myelination lead to peripheral neuropathies such as Charcot-Marie-Tooth disease and congenital hypomyelinating neuropathy (Brennan et al. 2015; Sanmaneechai et al. 2015; Scherer and Wrabetz 2008; Warner et al. 1999).

Peripheral myelin formation requires SC expansion and differentiation, and the onset of myelination is linked to cell cycle exit (Atanasoski et al. 2006; Jessen and Mirsky 2005). Controlling the balance between SC proliferation and differentiation is critical for ensuring myelination proceeds properly. The TSC1/2-mTOR signaling axis regulates cell growth and differentiation by regulating protein translation (Laplante and Sabatini 2009). Various upstream signals, such as nutrients and growth factors, converge on the tumor suppressors TSC1 and TSC2, which form a complex that negatively regulates the mTOR pathway, and ultimately organismal growth and homeostasis (Inoki et al. 2002; Laplante and Sabatini 2012). Disruption of the TSC1/2 complex activates Rheb-GTPase and subsequent mTOR signaling through the mTORC1 and mTORC2 complexes. mTOR targets S6K and 4EBP1 control cell growth processes such as ribosomal biogenesis and cap-dependent protein translation (Hay and Sonenberg 2004; Huang and Manning 2008).

SC growth and differentiation can be driven by extracellular molecules such as neuregulin I (NRG1) and laminin 211/GPR126, and intracellular signaling cascades including the Hippo and PI3K-AKT signaling pathways (D'Antonio et al. 2006; Deng et al. 2017; Ghidinelli et al. 2017; Herbert and Monk 2017; Monk et al. 2015; Taveggia et al. 2005). Activation of the

PI3K-AKT pathway by axonal NRG1 acts upstream of mTOR, regulating SC migration, proliferation, and survival (Ma et al. 2011; Maurel and Salzer 2000; Yamauchi et al. 2008). Balanced effects of cell-cycle promoting effectors and inhibitors, such as CDK2 and p27, respectively, regulate SC lineage progression (Porrello et al. 2014; Tikoo et al. 2000). In addition, mTOR signaling has also been implicated in regulation of the polo-like kinase (PLK) pathway (Nakashima et al. 2008; Renner et al. 2010). PLKs are key regulators of cell cycle progression with established functions in cell cycle entry, mitosis, bipolar spindle formation, chromosome segregation, and cytokinesis (Barr et al. 2004; Liu and Erikson 2002; Tang et al. 2006).

mTORC1 is crucial for myelination in both central and peripheral nervous systems (Beirowski et al. 2017; Bercury et al. 2014; Figlia et al. 2018; Lebrun-Julien et al. 2014; Norrmén et al. 2014; Sherman et al. 2012; Wahl et al. 2014). Loss of mTOR leads to profound hypomyelination in the PNS (Sherman et al. 2012), and, conversely, activation of mTOR through the loss of PTEN or activation of AKT promotes hypermyelination in the PNS (Domenech-Estevez et al. 2016; Goebbels et al. 2010; Maurel and Salzer 2000). Recent studies indicate that TSC1/2-mTOR signaling is a critical regulator of SC development and myelination in the PNS (Beirowski et al. 2017; Figlia et al. 2017), however, the precise mechanisms whereby mTOR controls SC growth and the transition from proliferation to differentiation are not yet fully understood.

Here, we show that sustained activation of mTOR signaling by *Tsc1* ablation during early developmental stages increased SC proliferation and delayed radial sorting, causing hypomyelination in the PNS, while *Tsc1* ablation in myelinating SCs at postnatal stages promoted myelin overgrowth and outfoldings. We further found that sustained signaling through the mTOR pathway led to activation of downstream PLK-mediated signaling. mTOR attenuation or pharmacological inhibition of PLK1/2 promotes SC differentiation and partially rescued myelination defects in *Tsc1*-mutant sciatic nerves. Our data suggest that the TSC1-mTOR-PLK axis maintains the homeostasis of SC proliferation and myelination in a stage-specific manner.

Materials and methods

Animals

The floxed *Tsc1* (*Tsc1*$^{fl/fl}$) mice (*Tsc1*<tm1Djk>/J – 005680; Jackson Laboratory) were crossed with *Dhh-Cre* mice to produce control (*Tsc1*$^{fl/+}$;*Cre*$^{+/-}$) and *Tsc1*-cKO offspring. *Tsc1*$^{fl/fl}$ mice were crossed with *Plp-creERT* (Jackson Laboratory, stock #005975) mice to produce control (*Tsc1*$^{fl/+}$;*Plp-CreERT*$^{+/-}$) and *Tsc1*-iKO offspring. Animals of both sexes were used in the study and heterozygous littermates were used as controls unless otherwise indicated. The mouse strains used in this study were generated and maintained on a mixed C57Bl/6;129Sv background and housed in a vivarium with a 12-hour light/dark cycle. All animal use protocols and studies were approved by the Institutional Animal Care and Use Committee of the Cincinnati Children's Hospital Medical Center.

Histology and electron microscopy

The sciatic nerves of mice at defined ages were dissected and fixed overnight in 4% paraformaldehyde and processed for cryo-sectioning or fiber analyses. Tissue processing was performed essentially as described previously (Wu et al. 2016). Briefly, mice were deeply anesthetized with ketamine/xylazine, perfused with 0.1 M cacodylate, followed by 2.5% paraformaldehyde/2.5% glutaraldehyde in 0.1 M cacodylate (pH 7.2). Sciatic nerves were dissected, post-fixed in 1% OsO_4, dehydrated through a graded ethanol series, infiltrated in propylene oxide, and embedded in resin. Semi-thin sections were stained with toluidine blue, and ultrathin sections were stained with lead citrate.

Immunohistochemistry and immunoblotting

Cryosections (8-μm thick) were permeabilized and blocked in blocking buffer (0.3% Triton X-100 and 5% normal donkey serum in PBS) for 1 h at room temperature and overlaid with primary antibodies overnight at 4 °C. Antibodies used in the study were goat anti-Sox10 (Santa Cruz Biotechnology, sc-17342), rabbit anti-Sox10 (Abcam, ab-25978-1000), goat anti-Oct6 (Santa Cruz Biotechnology, sc-11661), rabbit anti-Egr2 (Santa Cruz Biotechnology, sc-20690), goat anti-MBP (Santa Cruz Biotechnology, sc-13914), TSC1 (Pierce PA5-18506), Ki67 (Thermo Scientific, RM9106-SO), rat anti-BrdU (Abcam, ab6326), mouse anti-PLK1 (Santa Cruz Biotechnology, sc-17783), goat anti-Sox2 (Santa Cruz Biotechnology, sc-17320), P-S6 (Cell Signaling Technology, 2211), S6 (Cell Signaling Technology, 2217), p-4EBP1 (Cell Signaling Technology, 9451), α-Tubulin (Cell Signaling Technology, 2144) and mouse anti-GAPDH (Millipore, Mab374). After washing in PBS, cells or sections were incubated with secondary antibodies conjugated to Cy2, Cy3, or Cy5 (Jackson ImmunoResearch Laboratories) for 2 h at room temperature, stained in DAPI for 10 min, washed in PBS, and mounted with Fluoromount-G (SouthernBiotech). Cell images were quantified in a double-blinded manner.

For BrdU incorporation, 100 mg/kg BrdU were injected by IP. Two hours later, mice were harvested and processed for immunohistochemistry analysis. For immunoblotting, sciatic nerves were incubated in 1× Passive Lysis Buffer (Promega) supplemented with a protease inhibitor cocktail (1:200, Sigma). After western blotting, proteins were detected with appropriate secondary antibodies by using chemiluminescence with the ECL kit (Pierce) according to the instructions of the manufacturer.

PLK inhibitor treatment

PLK inhibitor BI-2536 (Biochempartner, 755038-02-9) was dissolved in ethanol and stored at a stock concentration of 10 mg/ml in aliquots at −20 °C. The working solution was prepared freshly before use at a final concentration of 1 mg/ml in 4% ethanol, 5% Tween 80, and 5% PEG400. Mice were administered daily intraperitoneal injections of either BI-2536 (5 mg/kg), as previously reported for in vivo treatment (Oueslati et al. 2013), or vehicle once per day from P7 to P14 or from P10 to P21. Mice were then harvested and analyzed by immunohistochemistry and ultrastructure analysis. For primary rat Schwann cell treatment, 100 nM BI-2536 working solution was mixed in the differentiation medium.

RNA extraction and qRT-PCR

Analyses were conducted with RNA extracts from a pool of sciatic nerve tissues of P7 mutant mice and their littermate controls. Total RNA was extracted per the Trizol (Life Technologies) protocol. cDNA was generated with iScript™ cDNA Synthesis Kit (Bio-Rad). qRT-PCR was performed using the ABI Prism 7700 Sequence Detector System (Perkin-Elmer Applied Biosystems). qRT-PCR primers for mouse gene sequences were PLK1-f, CAGCAAGTGGGTGGACTATT; PLK1-r, AGAGAATCAGGCGTGTTGAG; PLK2-f, GAGGACAGGATCTCTACAACTTTC; PLK2-r, AGAGCATGTTCAGGGCATATT; CDC25A-f, GACCAGTATTGCTGCTACTCAA; CDC25B-r, GGTCTGGGAAGGTTAGCTTATG; CDC25B1-f, CACCTCTCGGTCTTTGAGTTT; CDC25B-r, TGTGCATGGTCTGTGTAAGAG; CDC25C-f, CATTCAGATGGAGGAGGAAGAG; CDC25C-r, CACTGTGTCTGGGCTGATATAC; Cdk1-f, CTGTTTGGAGGATCTCGGTAAG; Cdk1-r, TTCCCTGACTCCAGCAAATG; GAPDH-f, ACCCAGAAGACTGTGGATGG; and GAPDH-r, CACATTGGGGGTAGGAACAC.

RNA-seq and data analysis

RNAs were isolated from the sciatic nerves of control mice and *Tsc1*$^{fl/+}$:*Dhh-Cre*$^{+/-}$ mutants at P7, and samples were subjected to RNA deep sequencing. RNA-seq libraries were prepared using Illumina RNA-seq Preparation Kit (Illumina) and sequenced on a HiSeq 2000 sequencer. RNA-seq reads were mapped using TopHat with default settings (http://tophat.cbcb.umd.edu). TopHat output data were then analyzed by Cufflinks to calculate FPKM values for known transcripts in the mouse genome reference and to test for differences in expression between *Tsc1*-cKO and control transcriptomes. Heatmap of gene differential expression was generated using Gene Cluster and Java Treeview. Gene ontology functional classifications were performed using DAVID (http://david.abcc.ncifcrf.gov) and Ingenuity Pathway Analysis.

Cell Cycle Analysis

One million purified rat Schwann cells per group were seeded onto 10 cm poly-L-lysine (PLL)-coated dishes and allowed to attach overnight. Cells were then treated with DMSO or 100 nM BI-2536 for 24 hrs. Cells were collected, fixed using cold 70% ethanol and stained with 7-AAD (7-amino actinomycin D). Stained cells were run on a BD™ LSR II flow cytometer and gated on forward and side scatter. Cell cycle distributions were computed using FlowJo platform (https://www.flowjo.com/)

Statistical analysis

All analyses were done using Microsoft Excel or GraphPad Prism 6.00 (www.graphpad.com). Quantifications were performed from at least three independent experiments. Data are shown as means ± SEM. Statistical significance ($p < 0.05$) was determined using two-tailed Student's t-tests unless otherwise indicated.

Accession codes—All the RNA-seq data have been deposited in the NCBI Gene Expression Omnibus (GEO) under accession number GSE 103957.

Results

TSC1 ablation in SC progenitors results in dysmyelination in the PNS

To determine how TSC1 functions in SC lineage development and myelination, we generated *Tsc1* knockout mice by crossing $Tsc1^{fl/fl}$ mice with the SC-expressing *Dhh-Cre* line (Figure 1a) (Jaegle et al. 2003). The $Tsc1^{fl/fl}$;$Dhh\text{-}Cre^{+/-}$ mice, referred to here as *Tsc1*-cKO mice, were born at normal Mendelian ratios and survived until around four months of age. We used either $Tsc1^{fl/fl}$ or $Tsc1^{fl/+}$;$Dhh\text{-}Cre^{+/-}$littermates as controls since they were phenotypically normal in SC development and myelination (Figure S1). Elimination of TSC1 expression was confirmed by immunostaining of teased fibers from sciatic nerves (Figure 1b). To examine whether *Tsc1* deletion resulted in hyperactivation of the mTOR pathway, we immunostained control and *Tsc1*-cKO sciatic nerves for phosphorylated ribosomal p70S6 (p-S6). At P10, the level of p-S6 expression was elevated in $Sox10^+$ SCs from *Tsc1*-cKO sciatic nerves (Figure 1c, d), suggesting that mTOR signaling is activated in the *Tsc1*-cKO mice. MBP expression was substantially decreased in *Tsc1*-cKO mice compared to their control littermates (Figure 1e, f), indicating a hypomyelination phenotype in the *Tsc1* mutant nerves. In contrast, we observed a robust increase of $Sox2^+$ immature SCs and a higher percentage of immature SCs in the SC lineage marked by Sox10 in the mutants compared to controls (Figure 1g, h). Since Sox2 expression reflects the SC progenitor state and subsides as differentiation commences, these observations suggest that *Tsc1* ablation in SC lineage progenitors inhibits the maturation process.

Lack of TSC1 elevates SC proliferation and blocks the differentiation process

The increase of $Sox2^+$/$Sox10^+$ immature SCs suggests that sustained mTOR activity may promote SC proliferation. We quantified SC proliferation in $Sox10^+$ SCs by immunolabeling with the proliferative marker Ki67 and using a BrdU incorporation in P10 sciatic nerves. BrdU labels proliferating cells in the S phase within two hours pulse-chasing, while Ki67 labels all cycling cells. Compared with the control nerves, the percentages of Ki67-expressing and BrdU-labeled proliferative SCs were significantly higher in *Tsc1*-mutant sciatic nerves than in controls (Figure 2a–d). This indicates that the activation of mTOR observed in the absence of TSC1 enhances SC proliferation.

At P10, control SCs had advanced to the myelinating phase, however, the percentage of $Krox20^+$ mature SCs was significantly reduced from 48 ± 2.0% in controls to 23 ± 1.1% in *Tsc1*-cKO sciatic nerves (Figure 2e, f). These data suggest that *Tsc1* ablation leads to an increase in proliferative SCs and a reduction in SC differentiation.

Tsc1-deficient mutants exhibit peripheral myelination defects

To examine the extent of myelination in *Tsc1*-cKO mice, we performed ultrastructural analysis at different stages by electron microscopy. At P7, SCs from control sciatic nerves had completed radial sorting and were present at a 1:1 ratio with axons; however, in *Tsc1*-cKO sciatic nerves, unmyelinated large axon bundles were detected (Figure 3a), suggesting a radial sorting defect in mutants. In contrast to control sciatic nerves where approximately 90% of axons were myelinated at P7, only approximately 6% of axons were myelinated in

Tsc1-cKO sciatic nerves (Figure 3a–c), indicating a defect in initiation of myelination in mutants (Figure 3a, c).

At P30, essentially all large diameter axons were myelinated in the control sciatic nerves. At this stage, approximately 90% of axons were myelinated in the *Tsc1*-cKO mutants, and the majority of SCs were present in a 1:1 ratio to axons (Figure 3d). However, we detected a substantial population of SCs that were not associated with axons and were not myelinating (Figure 3d, e), suggesting that these SCs are immature. The thickness of myelin sheath defined by the g-ratio (the ratio between inner axon diameter and outer diameter of the myelinated sheath) of sciatic nerve fibers (Hildebrand and Hahn 1978), however, was significantly lower in *Tsc1*-cKO mice than in control mice (Figure 3f).

At P60, the number of immature SCs that were not associated with axons in *Tsc1*-cKO mice was diminished, however, the percentage of unmyelinated axons was still higher in *Tsc1*-mutant sciatic nerves than controls (Figure 3g,h). The thickness of myelin sheath defined by the g-ratio of sciatic nerve fibers remained lower in *Tsc1*-cKO mice (Figure 3i). Together, these data showed that the *Tsc1*-cKO mice have a hypomyelinating phenotype during peripheral nerve development, indicating that ablation of *Tsc1* delays SC differentiation and myelination processes.

Myelin deficiency in *Tsc1*-cKO mice is dependent on mTOR signaling

Given that TSC1 is an upstream negative regulator of mTOR signaling (Laplante and Sabatini 2009), we hypothesized that hypomyelination seen in the *Tsc1*-cKO mutants is due to mTOR activation. To test this hypothesis, we generated a *Tsc1*-cKO model with a reduction of mTOR by carrying an mTOR floxed allele to complement the *Tsc1* mutation. SCs in heterozygous mice ($Tsc1^{fl/+}mTOR^{fl/+}$;*Dhh-Cre*) developed normally and had similar myelination profiles as wild-type mice (data not shown). We immunostained for the pro-myelinating marker Oct6 and mature SC marker Krox20 in the sciatic nerves from control, *Tsc1*-cKO, and $Tsc1^{fl/fl}mTOR^{fl/+}$;*Dhh-Cre* (hereafter referred to as *Tsc1*-cKO;$mTOR^{fl/+}$) mice at P30. In contrast to the reduction of $Krox20^{+}$ myelinating SCs (approximately 20% of controls) and the increase of pro-myelinating $Oct6^{+}$ immature SCs in *Tsc1*-cKO mice compared to controls, in *Tsc1*-cKO;$mTOR^{fl/+}$ mice, approximately 35% of myelinating SCs expressed Krox20 and the frequency of immature $Oct6^{+}$ SCs were lower following monoallelic loss of *mTOR* than in *Tsc1*-cKO mice (Figure 4a–c). These observations suggest that attenuation of mTOR activity in part reverses the SC differentiation block in *Tsc1*-cKO mice. We next evaluated the myelinogenesis in adult *Tsc1*-cKO;$mTOR^{fl/+}$ mice. The thickness of the myelin sheath assessed by *g*-ratio was increased in *Tsc1*-cKO;$mTOR^{fl/+}$ sciatic nerves compared with *Tsc1*-cKO mice (Figure 4d, e), suggesting that genetic attenuation of mTOR gene dosage restores dysmyelinating phenotype in *Tsc1*-cKO sciatic nerves.

Intriguingly, loss of both *mTOR* alleles in *Tsc1*-cKO mice (*Tsc1*-cKO;$mTOR^{fl/fl}$) led to a reduced myelin sheath thickness compared to *Tsc1*-cKO;$mTOR^{fl/+}$ mice even at P60 (Figure 4d, e), and a phenotype resembling that of *mTOR* mutants ($mTOR^{fl/fl}$;*Cnp1-Cre*) (Sherman et al. 2012), suggesting that mTOR is critical for normal SC myelination. Together, our data

suggest that dosage-dependent and balanced levels of TSC1-mTOR signaling is critical for proper SC differentiation and myelinogenesis.

Tsc1 loss in mature SCs leads to redundant myelin formation

To examine whether *Tsc1* deficiency leads to sustained myelination defects in *Tsc1*-cKO mutants, we analyzed the myelin ultrastructure in adulthood. The percentage of unmyelinated axons in the *Tsc1*-mutant sciatic nerves remained significantly higher at P122 compared to wild-type mice (Figure 5a, b). However, some myelinating axons in the mutant mice exhibited redundant myelin overgrowth, manifested as myelin outfoldings and recurrent myelin structures in *Tsc1*-cKO mutants (Figure 5c).

To determine the stage at which TSC1 functions in SC myelination, we inactivated *Tsc1* in mature SCs by using a tamoxifen-inducible SC-expressing *Plp-CreERT* driver (Doerflinger et al. 2003). This strategy bypasses the possible impact of the *Tsc1* loss early in SC development. The $Tsc1^{fl/fl}$:*Plp-CreERT* (*Tsc1*-iKO) mice were treated with tamoxifen from P30 for 10 days to induce deletion of *Tsc1* and analyzed at P120. Strikingly, *Tsc1*-iKO mice had thicker myelin in the sciatic nerves with a lower *g*-ratio compared with the $Tsc1^{fl/fl}$ control mice, and developed redundant myelin profiles (Figure 5d, e), indicating that activation of mTOR signaling in mature SCs enhances myelin sheath production. These observations suggest a stage-dependent function of TSC1 in SC proliferation and myelinogenesis and TSC1 as a sensor for myelin homeostasis in the PNS.

Tsc1 ablation in SC progenitors upregulates cell cycle regulators

To determine the downstream mediators of TSC1-mTOR signaling involved in SC proliferation and differentiation, we performed transcriptome profiling of control and *Tsc1*-cKO sciatic nerves at P7, which contain both proliferating and differentiating SCs. Gene ontology analysis revealed that differentially expressed genes were overrepresented for cell cycle, lipid biosynthesis, and myelination (Figure 6a). Downregulated genes in *Tsc1*-cKO nerves were associated with SC differentiation, myelination and lipid biosynthesis programs (Svaren and Meijer 2008), while upregulated genes were linked to cell cycle, cell proliferation and mitosis (Figure 6b). This is consistent with the aberrant increase of cell proliferation and the dysmyelination phenotype in *Tsc1*-cKO mice.

We further identified an altered gene cluster related to cell proliferation that is overrepresented in the Polo-like kinase (PLK) pathway, cell-cycle regulation, and G1/S checkpoint signaling (Figure 6b). Activation of PLK1 and PLK2 promotes cell-cycle progression (Archambault and Glover 2009; van de Weerdt and Medema 2006). We examined the mRNA levels of *Plk1* and *Plk2* and other known cell cycle regulators *Cdc25A*, *Cdc25B*, and *Cdc25C* by qRT-PCR and found that *Plk1/2* mRNAs were substantially elevated in *Tsc1*-cKO sciatic nerves compared to controls (Figure 6c). Western blot analysis confirmed the increase of PLK1 levels as well as increases in p-S6 and p-4EBP1 expression caused by mTOR activation in *Tsc1*-cKO sciatic nerves as compared to control nerves at P10 (Figure 6d), although a suitable PLK2 antibody is not available. These data suggest that *Tsc1* loss activates the cell proliferation program in SCs.

To determine whether activation of this PLK1 pathway can be induced in mature Schwann cells of adult sciatic nerves upon *Tsc1* deletion, we performed a western blot analysis of PLK1 expression in sciatic nerves from *Tsc1*-iKO mice, which were injected with tamoxifen at the young adult stage P30 and harvested at P60. Our results indicate that PLK1 levels increase following Tsc1 knockout in mature Schwann cells in adult sciatic nerves (Figure 6e, f). Therefore, upregulation of the PLK1 pathway can be induced by mTOR signaling at both perinatal and adult stages.

Tsc1 ablation-induced hypomyelination is dependent on Polo-like kinase signaling

To address how expression of *Plk1* changes during sciatic nerve development, we performed qRT-PCR to examine the *Plk1* mRNA levels at P0, P14 and P28. *Plk1* expression is highest at P0 and decreases over development as myelinating Schwann cells mature (Figure 7a). To determine whether SC hyperproliferation in *Tsc1*-cKO sciatic nerves is dependent on PLK activity, we treated rat SCs with BI-2536, which preferentially inhibits both PLK1 and PLK2 (Inglis et al. 2009; Lenart et al. 2007; Oueslati et al. 2013). Rat SCs treated with the PLK inhibitor-BI2536 were unable to recruit alpha-tubulin to centrosomes and did not form bipolar mitotic spindles (Figure 7b), consistent with the critical role of PLK1/2 in cell cycle progression and mitosis. To investigate if PLK signaling regulates Schwann cell progression through the G2/M transition, we performed cell cycle analysis using 7-AAD in rat Schwann cells exposed to PLK inhibitor or vehicle. We found that rat Schwann cells treated with PLK inhibitor BI2536 resulted in an accumulation of cells in G2 phase and a decreased fraction of cells in S phase as assessed by fluorescence-activated cell sorting analysis. This suggests that PLK signaling activity has a role in promoting the G2/M transition during cell cycle progression in Schwann cells (Figure 7c).

To further investigate the effects of PLK inhibition on SC development in *Tsc1*-cKO mice, we treated *Tsc1*-cKO mice with or without PLK1/2 inhibitor BI-2536 from P7 to P14. Treatment with BI-2536 reduced the proliferation rate of SCs in the sciatic nerves of *Tsc1*-cKO mice (Figure 7d, e). BI2536 treatment increased expression of the mature SC marker MBP in *Tsc1*-cKO sciatic nerves compared with vehicle-treated nerves (Figure 7f). The percentage of $Krox20^+$ mature SCs among $Sox10^+$ SCs increased from approximately 23% in the vehicle-treated group to about 65% in BI2536-treated group (Figure 7g, h). Consistently, ultrastructural analysis further indicated that the percentage of myelinated axons as well as myelin thickness in the BI2536-treated *Tsc1*-cKO mutants at P21 were significantly greater than those in the vehicle-treated group (Figure 7i–k).

Thus, inhibition of PLK signaling at least partially restores the SC differentiation and myelination program by dampening excessive proliferation of immature SCs in *Tsc1*-cKO sciatic nerves. The complementation suggests that activation of the PLK pathway contributes to the excessive SC proliferation that culminates at the expense of SC differentiation in *Tsc1*-cKO mutants.

Discussion

TSC1 functions stage-specifically in SC proliferation and myelinogenesis

mTOR signaling is required for myelination in the peripheral nervous system (Norrmén et al. 2014; Sherman et al. 2012). The effect of activation of mTOR signaling on SC development has been examined through perturbations in *Pten* and in *Akt*, genes encoding upstream regulators of mTOR signaling (Domenech-Estevez et al. 2016; Flores et al. 2008; Goebbels et al. 2010). Recent studies indicate that mTOR hyperactivation caused by *Tsc2* or *Tsc1* deletion altered SC developmental programs, and delayed the onset of SC myelination and remyelination after nerve injury (Beirowski et al. 2017; Figlia et al. 2017). In contrast to mice in which *Tsc1* was ablated at P0 using the Cre system, which exhibit minor developmental defects in sciatic nerves (Beirowski et al. 2017), in the present study we found that mice in which *Tsc1* was deleted in SC precursors using *Dhh-Cre* expressed at E12.5 exhibited extensive hyperproliferation of immature SCs in the developing nerves. *Dhh-Cre* expression begins one day earlier than that of P0-Cre (Feltri et al. 1999; Jaegle et al. 2003), which could account for this discrepancy. This suggests that TSC1-mediated regulation of SC proliferation is important at this early stage of immature SC development and that timing of mTOR activation is critical for SC expansion, in keeping with data from others (Figlia et al. 2017). In *Tsc1*-cKO mutants, SC over-proliferation and persistence of the immature state contribute to the block of differentiation at the pro-myelinating stage and delaying the myelination process. We did not observe any significant difference of myelin formation and SC numbers in sciatic nerves between heterozygous $Tsc1^{fl/+}$;$Dhh\text{-}Cre^{+/-}$ and $Tsc1^{fl/fl}$ mice, suggesting a dose-dependent TSC1-mTOR signaling in regulating SC development.

Strikingly, adult *Tsc1*-cKO mutant nerves developed redundant myelin and focal hypermyelination, in keeping with *Tsc1* P0-Cre mutants in adulthood (Beirowski et al. 2017). *Tsc1* ablation in mature SCs induced by *Plp-CreERT* at the young adult stage also resulted in hypermyelination of peripheral nerves. This is consistent with previous reports that activation of PI3K-mTOR signaling could reinitiate myelin synthesis in mature SCs (Goebbels et al. 2010; Snaidero et al. 2014). Our data support the notion that the TSC1-mTOR signaling pathway acts as a signal to limit myelin sheath growth in mature SCs following wrapping and that the loss of this signal drives myelin expansion. Thus, together with reported studies, these data indicate that TSC1-mTOR signaling executes dosage- and stage-specific functions to regulate SC proliferation, differentiation and myelinogenesis at multiple levels.

Distinct and context-dependent requirements for TSC1-mTOR signaling in central and peripheral myelinogenesis

In contrast to the central nervous system, where sustained activation of mTOR in oligodendrocyte progenitors in *Tsc1* mutants leads to oligodendrocyte cell death and myelination defects with minimal impact on oligodendrocyte progenitor proliferation (Jiang et al. 2016), *Tsc1* deletion in the SC lineage leads to an increase in SC proliferation and consequent arrest of the SC differentiation process without triggering substantial cell loss.

These results suggest a distinct cell-type specific function of TSC1-mTOR signaling in oligodendrocyte and SC development.

Differential responses with respect to cell survival and differentiation in oligodendrocytes and SCs following *Tsc1* deletion suggest that the complex function of TSC1-mTOR is context-dependent. Despite similar downregulation of myelination-associated genes in *Tsc1*-deleted SCs and oligodendrocytes, there are striking differences in differentially expressed genes and regulatory pathways. In the central white matter tracts, the most prominent elevated pathways in oligodendrocytes are related to regulation of endoplasmic reticulum (ER) stress, apoptosis, and the inflammatory response, whereas in SCs cell cycle-related pathways, cyclin-dependent pathways, and polo-like kinase signaling are upregulated substantially in SCs, suggesting intrinsic differences between oligodendrocytes and SCs in responses to sustained mTOR activation in *Tsc1* mutants or distinct microenvironments.

In the central nervous system, sustained activation of mTOR signaling leads to ER stress and oligodendrocyte cell death, whereas in peripheral nerves, despite the increase in ER stress responses (Figure S2), excessive mTOR signaling activation promotes proliferation of immature SCs unchecked by apoptosis. Although the molecular mechanisms underlying distinct phenotypes in the central and peripheral nervous systems remain to be elucidated, elevation of adaptive responses mediated by p-eIF2α (Jiang et al. 2016; Way et al. 2015) in *Tsc1*-mutant SCs (Figure S2) and strong upregulation of the SC proliferative program may contribute to SC survival.

TSC1-mTOR signaling activates PLK to promote SC proliferation

Although the recent studies focus on SC myelination (Beirowski et al. 2017; Figlia et al. 2017), the molecular mechanisms underlying TSC1 function in SC proliferation have not been fully defined. mTOR signaling regulates both cell cycle progression and cell growth mainly by controlling protein translation through the downstream effectors S6K and 4E-BP1 (Astrinidis et al. 2006; Miloloza et al. 2000; Zacharek et al. 2005). mTORC1 activity appears to activate S6K to negatively regulate Krox20, a key SC regulator, to forestall the onset of SC myelination (Figlia et al. 2017). We observed an increase in the proliferation of immature SCs and in expression of p-S6K and p-4E-BP1 in *Tsc1*-cKO mutants at early developmental stages, when SCs undergo proliferation. The attenuation of mTOR activity in *Tsc1*-cKO;$mTOR^{f/+}$ mice decreased SC proliferation and partially restored the number of myelinated fibers, consistent with a recent study involving treatment of $Tsc1^{fl/fl}$;*P0-Cre* mice with rapamycin, a pharmacological mTOR inhibitor (Beirowski et al. 2017; Figlia et al. 2017). These observations suggest that the SC hyperproliferation and differentiation block observed upon ablation of *Tsc1* is mediated through mTOR activity.

Strikingly, our transcriptome profiling analyses revealed a substantial upregulation of *PLK1/2* expression in developing *Tsc1*-mutant sciatic nerves, in addition to the downregulation of myelination-associated programs. Polo-like kinases such as PLK1 and PLK2 are essential for cell proliferation and mitosis (Archambault and Glover 2009). PLK1/2 promote mitotic entry by phosphorylating cyclin B1 and CDK1 and initiate cytokinesis by activating the anaphase promoting complex (Archambault and Glover 2009; Barr et al. 2004; Strebhardt 2010). Due to their mitotic function and overexpression in

cancers, inhibitors of PLKs are currently being evaluated in clinical trials (Janning and Fiedler 2014; Muller-Tidow et al. 2013). We found that pharmacological inhibition of PLK1/2 reduced SC over-proliferation and, at least in part, rescued the myelination defect caused by the *Tsc1* loss in peripheral nerves. This provides evidence that PLK1/2 function as downstream mediators for TSC1-mTOR signaling to regulate the transition from proliferation to differentiation during SC lineage progression. Given that the mTOR pathway is regulated by upstream PI3K-Akt signaling, stage-specific modulation of PI3K-Akt-mTOR activity and the downstream PLK signaling pathway may permit the proper control of SC proliferation and regeneration, while promoting SC differentiation and remyelination in inherited and acquired demyelinating peripheral neuropathies.

Supplementary Material

Refer to Web version on PubMed Central for supplementary material.

Acknowledgments

Authors would like to thank Brad Meyer and Zhixing Ma for technical support. We thank Dr. Edward Hurlock for comments. This study was funded in part by grants from the US National Institutes of Health R01NS072427 and R01NS075243 to QRL and the National Multiple Sclerosis Society (NMSS-4727) to QRL, and R01NS062796 to J.R.C. and National Natural Science Foundation of China NSFC 31271134 to Hu.W.

References

Archambault V, Glover DM. Polo-like kinases: conservation and divergence in their functions and regulation. Nat Rev Mol Cell Biol. 2009; 10:265–75. [PubMed: 19305416]

Atanasoski S, Boller D, De Ventura L, Koegel H, Boentert M, Young P, Werner S, Suter U. Cell cycle inhibitors p21 and p16 are required for the regulation of Schwann cell proliferation. Glia. 2006; 53:147–57. [PubMed: 16206162]

Barr FA, Sillje HH, Nigg EA. Polo-like kinases and the orchestration of cell division. Nat Rev Mol Cell Biol. 2004; 5:429–40. [PubMed: 15173822]

Beirowski B, Wong KM, Babetto E, Milbrandt J. mTORC1 promotes proliferation of immature Schwann cells and myelin growth of differentiated Schwann cells. Proc Natl Acad Sci U S A. 2017; 114:E4261–E4270. [PubMed: 28484008]

Bercury KK, Dai JX, Sachs HH, Ahrendsen JT, Wood TL, Macklin WB. Conditional Ablation of Raptor or Rictor Has Differential Impact on Oligodendrocyte Differentiation and CNS Myelination. Journal of Neuroscience. 2014; 34:4466–4480. [PubMed: 24671993]

Brennan KM, Bai Y, Shy ME. Demyelinating CMT--what's known, what's new and what's in store? Neurosci Lett. 2015; 596:14–26. [PubMed: 25625223]

D'Antonio M, Droggiti A, Feltri ML, Roes J, Wrabetz L, Mirsky R, Jessen KR. TGFbeta type II receptor signaling controls Schwann cell death and proliferation in developing nerves. J Neurosci. 2006; 26:8417–27. [PubMed: 16914667]

Deng Y, Wu LMN, Bai S, Zhao C, Wang H, Wang J, Xu L, Sakabe M, Zhou W, Xin M, et al. A reciprocal regulatory loop between TAZ/YAP and G-protein Galphas regulates Schwann cell proliferation and myelination. Nat Commun. 2017; 8:15161. [PubMed: 28443644]

Doerflinger NH, Macklin WB, Popko B. Inducible site-specific recombination in myelinating cells. Genesis. 2003; 35:63–72. [PubMed: 12481300]

Domenech-Estevez E, Baloui H, Meng X, Zhang Y, Deinhardt K, Dupree JL, Einheber S, Chrast R, Salzer JL. Akt Regulates Axon Wrapping and Myelin Sheath Thickness in the PNS. J Neurosci. 2016; 36:4506–21. [PubMed: 27098694]

Figlia G, Gerber D, Suter U. Myelination and mTOR. Glia. 2018; 66:693–707. [PubMed: 29210103]

Figlia G, Norrmen C, Pereira JA, Gerber D, Suter U. Dual function of the PI3K-Akt-mTORC1 axis in myelination of the peripheral nervous system. Elife. 2017:6.

Ghidinelli M, Poitelon Y, Shin YK, Ameroso D, Williamson C, Ferri C, Pellegatta M, Espino K, Mogha A, Monk K, et al. Laminin 211 inhibits protein kinase A in Schwann cells to modulate neuregulin 1 type III-driven myelination. PLoS Biol. 2017; 15:e2001408. [PubMed: 28636612]

Goebbels S, Oltrogge JH, Kemper R, Heilmann I, Bormuth I, Wolfer S, Wichert SP, Mobius W, Liu X, Lappe-Siefke C, et al. Elevated phosphatidylinositol 3,4,5-trisphosphate in glia triggers cell-autonomous membrane wrapping and myelination. J Neurosci. 2010; 30:8953–64. [PubMed: 20592216]

Hay N, Sonenberg N. Upstream and downstream of mTOR. Genes Dev. 2004; 18:1926–45. [PubMed: 15314020]

Herbert AL, Monk KR. Advances in myelinating glial cell development. Curr Opin Neurobiol. 2017; 42:53–60. [PubMed: 27930937]

Hildebrand C, Hahn R. Relation between myelin sheath thickness and axon size in spinal cord white matter of some vertebrate species. J Neurol Sci. 1978; 38:421–34. [PubMed: 310448]

Huang J, Manning BD. The TSC1-TSC2 complex: a molecular switchboard controlling cell growth. Biochem J. 2008; 412:179–90. [PubMed: 18466115]

Inglis KJ, Chereau D, Brigham EF, Chiou SS, Schobel S, Frigon NL, Yu M, Caccavello RJ, Nelson S, Motter R, et al. Polo-like kinase 2 (PLK2) phosphorylates alpha-synuclein at serine 129 in central nervous system. J Biol Chem. 2009; 284:2598–602. [PubMed: 19004816]

Inoki K, Li Y, Zhu T, Wu J, Guan KL. TSC2 is phosphorylated and inhibited by Akt and suppresses mTOR signalling. Nat Cell Biol. 2002; 4:648–57. [PubMed: 12172553]

Jaegle M, Ghazvini M, Mandemakers W, Piirsoo M, Driegen S, Levavasseur F, Raghoenath S, Grosveld F, Meijer D. The POU proteins Brn-2 and Oct-6 share important functions in Schwann cell development. Genes Dev. 2003; 17:1380–91. [PubMed: 12782656]

Jessen KR, Mirsky R. The origin and development of glial cells in peripheral nerves. Nature reviews Neuroscience. 2005; 6:671–82. [PubMed: 16136171]

Laplante M, Sabatini DM. mTOR signaling at a glance. Journal of Cell Science. 2009; 122:3589–3594. [PubMed: 19812304]

Laplante M, Sabatini DM. mTOR signaling in growth control and disease. Cell. 2012; 149:274–93. [PubMed: 22500797]

Lebrun-Julien F, Bachmann L, Norrmen C, Trotzmuller M, Kofeler H, Ruegg MA, Hall MN, Suter U. Balanced mTORC1 activity in oligodendrocytes is required for accurate CNS myelination. J Neurosci. 2014; 34:8432–48. [PubMed: 24948799]

Lenart P, Petronczki M, Steegmaier M, Di Fiore B, Lipp JJ, Hoffmann M, Rettig WJ, Kraut N, Peters JM. The small-molecule inhibitor BI 2536 reveals novel insights into mitotic roles of polo-like kinase 1. Curr Biol. 2007; 17:304–15. [PubMed: 17291761]

Liu X, Erikson RL. Activation of Cdc2/cyclin B and inhibition of centrosome amplification in cells depleted of Plk1 by siRNA. Proc Natl Acad Sci U S A. 2002; 99:8672–6. [PubMed: 12077309]

Ma Z, Wang J, Song F, Loeb JA. Critical period of axoglial signaling between neuregulin-1 and brain-derived neurotrophic factor required for early Schwann cell survival and differentiation. J Neurosci. 2011; 31:9630–40. [PubMed: 21715628]

Maurel P, Salzer JL. Axonal regulation of Schwann cell proliferation and survival and the initial events of myelination requires PI 3-kinase activity. J Neurosci. 2000; 20:4635–45. [PubMed: 10844033]

Monk KR, Feltri ML, Taveggia C. New insights on Schwann cell development. Glia. 2015; 63:1376–93. [PubMed: 25921593]

Nakashima A, Maruki Y, Imamura Y, Kondo C, Kawamata T, Kawanishi I, Takata H, Matsuura A, Lee KS, Kikkawa U, et al. The yeast Tor signaling pathway is involved in G2/M transition via polo-kinase. PLoS One. 2008; 3:e2223. [PubMed: 18493323]

Norrmén C, Figlia G, Lebrun-Julien F, Pereira JA, Trötzmüller M, Köfeler HC, Rantanen V, Wessig C, van Deijk A-LF, Smit AB, et al. mTORC1 controls PNS myelination along the mTORC1-RXRγ-SREBP-lipid biosynthesis axis in Schwann cells. Cell reports. 2014; 9:646–60. [PubMed: 25310982]

Oueslati A, Schneider BL, Aebischer P, Lashuel HA. Polo-like kinase 2 regulates selective autophagic alpha-synuclein clearance and suppresses its toxicity in vivo. Proc Natl Acad Sci U S A. 2013; 110:E3945–54. [PubMed: 23983262]

Porrello E, Rivellini C, Dina G, Triolo D, Del Carro U, Ungaro D, Panattoni M, Feltri ML, Wrabetz L, Pardi R, et al. Jab1 regulates Schwann cell proliferation and axonal sorting through p27. J Exp Med. 2014; 211:29–43. [PubMed: 24344238]

Renner AG, Creancier L, Dos Santos C, Fialin C, Recher C, Bailly C, Kruczynski A, Payrastre B, Manenti S. A functional link between polo-like kinase 1 and the mammalian target-of-rapamycin pathway? Cell Cycle. 2010; 9:1690–6. [PubMed: 20404504]

Sanmaneechai O, Feely S, Scherer SS, Herrmann DN, Burns J, Muntoni F, Li J, Siskind CE, Day JW, Laura M, et al. Genotype-phenotype characteristics and baseline natural history of heritable neuropathies caused by mutations in the MPZ gene. Brain. 2015; 138:3180–92. [PubMed: 26310628]

Scherer SS, Wrabetz L. Molecular mechanisms of inherited demyelinating neuropathies. Glia. 2008; 56:1578–89. [PubMed: 18803325]

Sherman DL, Krols M, Wu L-MN, Grove M, Nave K-A, Gangloff Y-G, Brophy PJ. Arrest of myelination and reduced axon growth when Schwann cells lack mTOR. The Journal of neuroscience : the official journal of the Society for Neuroscience. 2012; 32:1817–25. [PubMed: 22302821]

Svaren J, Meijer D. The molecular machinery of myelin gene transcription in Schwann cells. Glia. 2008; 56:1541–51. [PubMed: 18803322]

Tang J, Erikson RL, Liu X. Ectopic expression of Plk1 leads to activation of the spindle checkpoint. Cell Cycle. 2006; 5:2484–8. [PubMed: 17102638]

Taveggia C, Zanazzi G, Petrylak A, Yano H, Rosenbluth J, Einheber S, Xu X, Esper RM, Loeb JA, Shrager P, et al. Neuregulin-1 type III determines the ensheathment fate of axons. Neuron. 2005; 47:681–94. [PubMed: 16129398]

Tikoo R, Zanazzi G, Shiffman D, Salzer J, Chao MV. Cell cycle control of Schwann cell proliferation: role of cyclin-dependent kinase-2. J Neurosci. 2000; 20:4627–34. [PubMed: 10844032]

van de Weerdt BC, Medema RH. Polo-like kinases: a team in control of the division. Cell Cycle. 2006; 5:853–64. [PubMed: 16627997]

Wahl SE, McLane LE, Bercury KK, Macklin WB, Wood TL. Mammalian target of rapamycin promotes oligodendrocyte differentiation, initiation and extent of CNS myelination. J Neurosci. 2014; 34:4453–65. [PubMed: 24671992]

Warner LE, Garcia CA, Lupski JR. Hereditary peripheral neuropathies: clinical forms, genetics, and molecular mechanisms. Annual review of medicine. 1999; 50:263–75.

Wu LM, Wang J, Conidi A, Zhao C, Wang H, Ford Z, Zhang L, Zweier C, Ayee BG, Maurel P, et al. Zeb2 recruits HDAC-NuRD to inhibit Notch and controls Schwann cell differentiation and remyelination. Nat Neurosci. 2016; 19:1060–72. [PubMed: 27294509]

Yamauchi J, Miyamoto Y, Chan JR, Tanoue A. ErbB2 directly activates the exchange factor Dock7 to promote Schwann cell migration. J Cell Biol. 2008; 181:351–65. [PubMed: 18426980]

Main points

Tumor Suppressor TSC1 has stage-dependent functions in Schwann cell proliferation and myelinogenesis. TSC1 regulates polo-like kinase expression for Schwann cell proliferation, while TSC1 loss in mature cells leads to overgrown myelin sheaths.

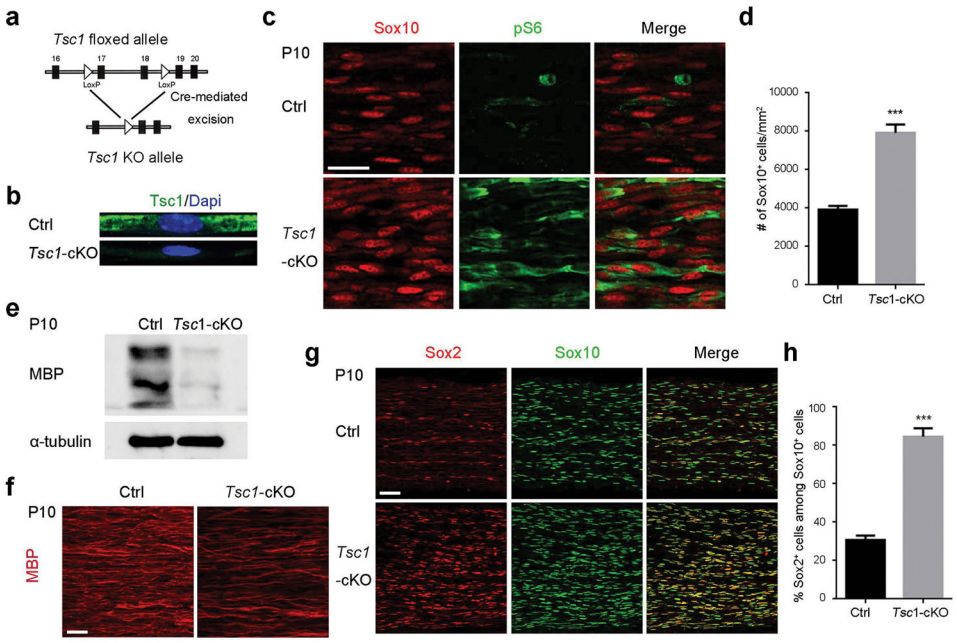

Figure 1. Ablation of *Tsc1* leads to hypomyelination

(a) Diagram of strategy for deletion of exons 17 and 18 of *Tsc1* by Dhh-Cre expressed specifically at E12.5 in Schwann cells.

(b) Representative images of *Tsc1*-cKO and control teased fibers of sciatic nerves at P10 stained for TSC1 and nuclei (with DAPI).

(c) Representative images of Sox10 and p-S6 staining of control and *Tsc1*-cKO sciatic nerves at P10. Scale bar, 15 μm.

(d) Quantification of $Sox10^+$ Schwann cells per mm^2 (n = 6 animals/genotype). Student's *t*-test, *** $p<0.001$.

(e) Representative western blot showing MBP expression in *Tsc1*-cKO mutant and control littermate at P10

(f) Representative images of control and *Tsc1*-cKO sciatic nerves at P10 stained for MBP. Scale bar, 25 μm.

(g) Representative images showing Sox2 and Sox10 staining of control and *Tsc1*-cKO mutants at P10. Scale bar, 50 μm.

(h) Quantification of percentages of $Sox2^+$ cells among $Sox10^+$ Schwann cells (n = 6 animals/genotype). Student's *t*-test, *** $p<0.001$.

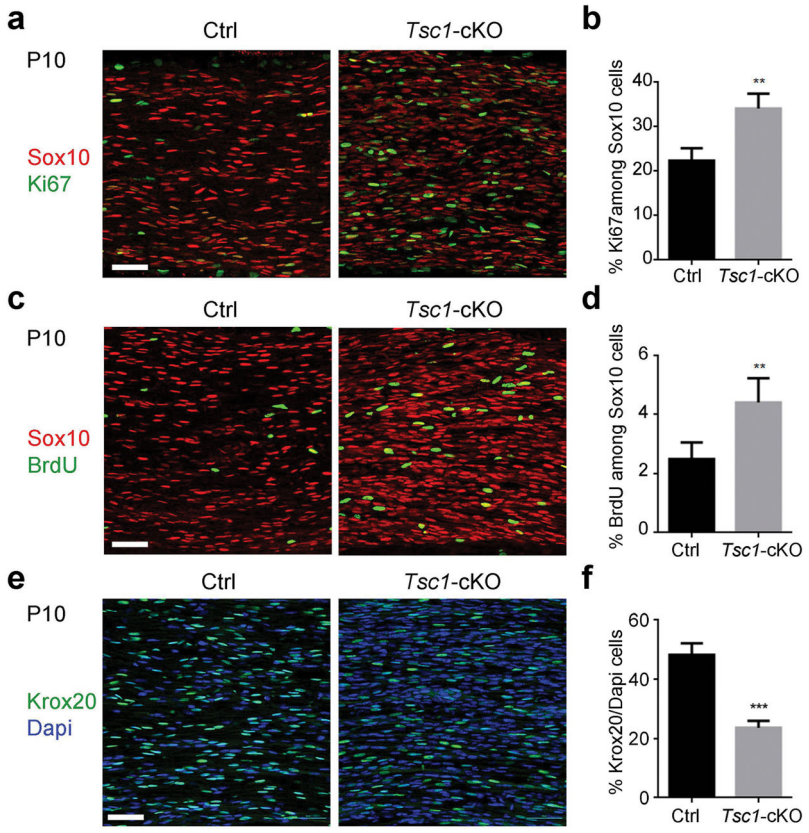

Figure 2. mTOR activation in *Tsc1* mutant mice promotes Schwann cell proliferation and blocks differentiation at the pro-myelin stage

(a) Representative images control and *Tsc1*-cKO sciatic nerves at P10 immunostained for Sox10 and Ki67. Scale bar, 50 μm.

(b) Quantification of cells expressing both Ki67 and Sox10 in control and *Tsc1*-cKO sciatic nerves (n = 6 animals/genotype). Student's *t*-test, **p<0.01.

(c) Representative images P10 control and *Tsc1*-cKO sciatic nerves stained for Sox10 and labeled with BrdU. Scale bar, 50 μm.

(d) Quantification of cells expressing both BrdU and Sox10 in control and *Tsc1*-cKO sciatic nerves (n = 6 animals/genotype). Student's *t*-test, **p<0.01.

(e) Representative images showing Krox20 expression in control and *Tsc1*-cKO sciatic nerves at P10. Scale bar, 50 μm.

(f) Percentages of Krox20^{+} cells in P10 control and *Tsc1*-cKO sciatic nerves (n = 6 animals/genotype). Student's *t*-test, *** p<0.001.

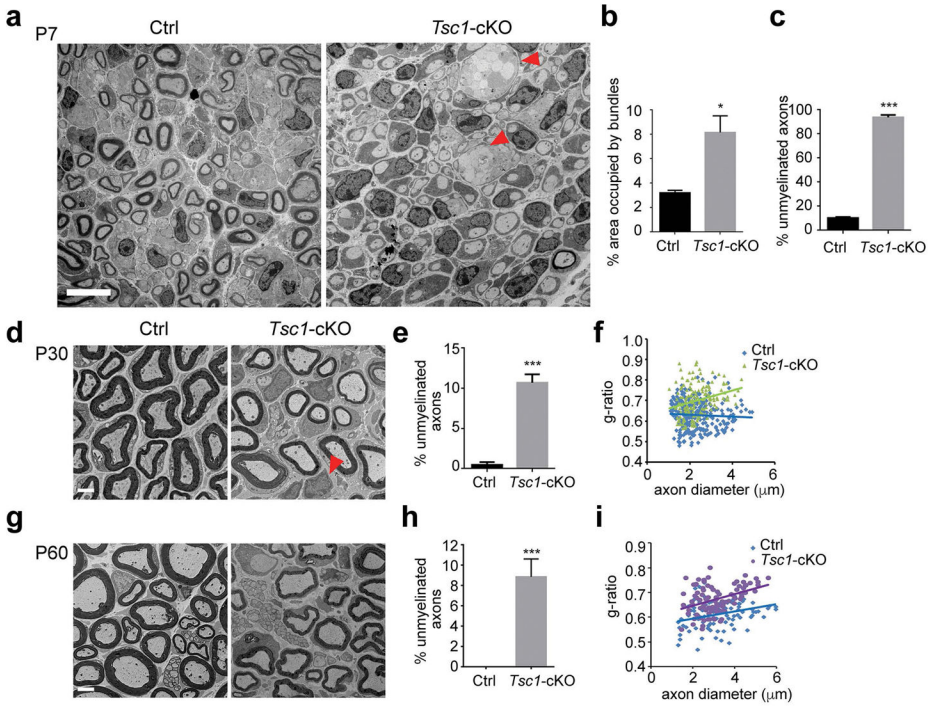

Figure 3. Ablation of *Tsc1* delays radial sorting and myelinogenesis

(a) Representative electron micrographs showing ultrastructure of sciatic nerves in control and *Tsc1*-cKO at P7. Unmyelinated large axon bundles are indicated with an arrowhead. Scale bar, 10 μm.

(b) Quantification of the areas of large bundles in control and *Tsc1*-cKO sciatic nerves at P7. n = 3 animals/genotype. Student's *t*-test, * $p<0.05$

(c) The percentages of unmyelinated axons in P7 control and *Tsc1-cKO* sciatic nerves. n = 3 animals/genotype. Student's *t*-test, *** $p<0.001$.

(d) Electron micrographs showing the ultrastructure of sciatic nerves from control and *Tsc1*-cKO mice at P30. Arrowheads indicate SCs that are not associated with axons. Scale bar, 2 μm.

(e) Quantification of percentages of unmyelinated axons in P30 control and *Tsc1*-cKO sciatic nerves. n = 3 animals/genotype. Student's *t*-test, *** $p<0.001$.

(f) Quantification of g-ratios of P30 control and *Tsc1*-cKO sciatic nerves. n = 3 animals/genotype. Student's *t*-test, *** $p<0.001$.

(g) Electron micrographs showing ultrastructure of sciatic nerves from control and *Tsc1*-cKO mice P60. Scale bar, 2 μm.

(h) Quantification of percentages of unmyelinated axons in P60 control and *Tsc1*-cKO sciatic nerves. n = 3 animals/genotype. Student's t-test, *** $p<0.001$.

(i) Quantification of g-ratios of P60 control and *Tsc1*-cKO sciatic nerves. n = 3 animals/genotype. Student's *t*-test, *** $p<0.001$.

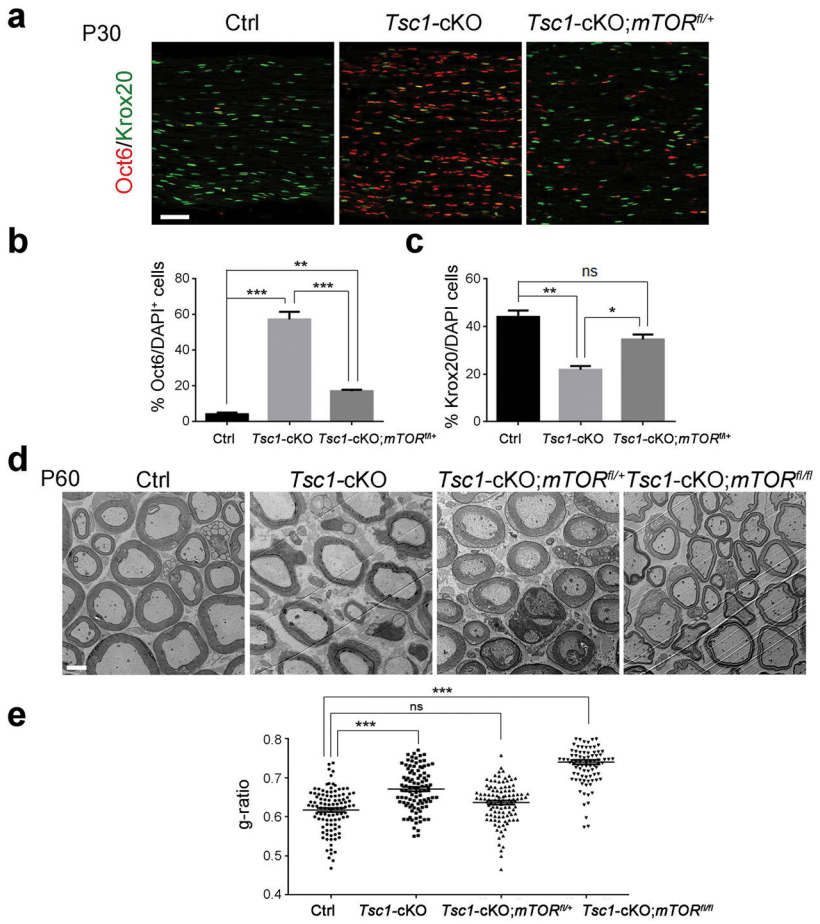

Figure 4. Reduction of mTOR rescues myelin defect in *Tsc1*-cKO mice

(a) Immunostained Oct6 and Krox20 in P30 sciatic nerves from control, *Tsc1*-cKO, and *Tsc1*-cKO;$mTOR^{fl/+}$ sciatic nerves. Scale bar, 50 μm.

(b) Quantification of percentages of $Oct6^{+}$ cells in control, *Tsc1*-cKO, and *Tsc1*-cKO;$mTOR^{fl/+}$ sciatic nerves. n = 3 animals/genotype. One way ANOVA with Tukey's *t*-test used to determine significance.

(c) Quantification of percentages of $Krox20^{+}$ cells in control, *Tsc1*-cKO, and *Tsc1*-cKO;$mTOR^{fl/+}$ sciatic nerves. n = 3 animals/genotype. One way ANOVA with Tukey's t-test used to determine significance.

(d) Representative electron micrographs of ultrastructure from P60 control, *Tsc1*-cKO, *Tsc1*-cKO;$mTOR^{fl/+}$ and *Tsc1*-cKO;$mTOR^{fl/fl}$. Scale bar, 2 μm.

(e) Quantification of g-ratios in P60 control, *Tsc1*-cKO *Tsc1*-cKO;$mTOR^{fl/+}$, *Tsc1*-cKO;$mTOR^{fl/fl}$ sciatic nerves (n > 200 myelinated axons from 3 mice per group). One way ANOVA with Tukey's *t*-test used to determine significance.

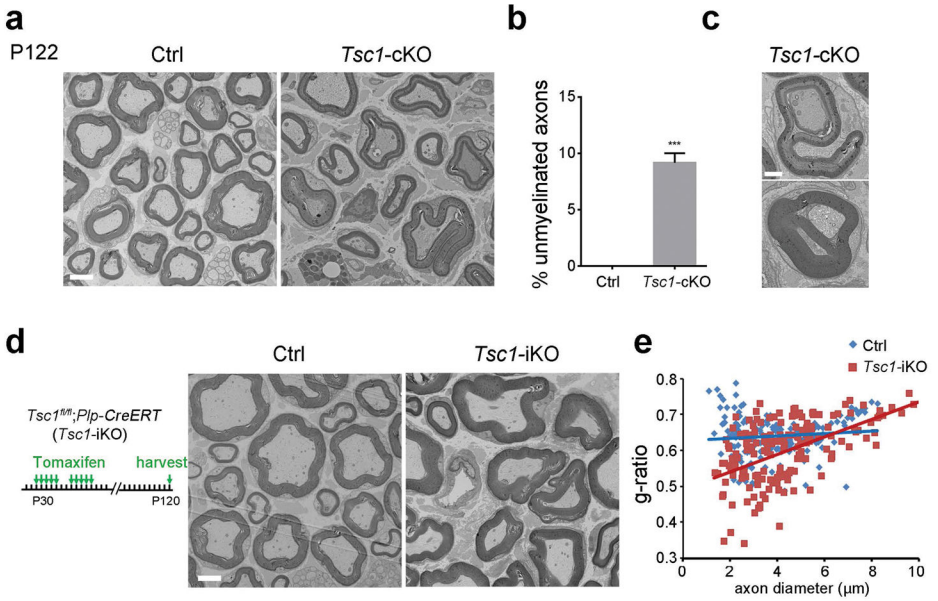

Figure 5. Lack of TSC1 leads to redundant myelin sheath formation in adulthood

(a) Representative electron micrographs of P122 control *Tsc1*$^{fl/fl}$ and *Tsc1*-cKO sciatic nerves. Scale bar, 2 μm.

(b) The percentages of unmyelinated axons in P122 control and *Tsc1*-cKO sciatic nerves. n = 3 animals/genotype. Student's *t*-test, *** p<0.001.

(c) High magnification electron micrographs showing redundant myelin in P122 *Tsc1*-cKO sciatic nerves. Scale bar, 800 nm.

(d) Left: Diagram showing tamoxifen administration to control (*Tsc1*$^{fl/fl}$) and *Tsc1*-iKO mice for 10 days followed by tissue collection at P120. Right: Representative electron micrographs of *Tsc1*$^{fl/fl}$ control and *Tsc1*-iKO sciatic nerves of mice after tamoxifen treatment at P120. Scale bar, 2 μm.

(e) Quantification of g-ratio in control and *Tsc1*-iKO sciatic nerves (n > 200 axons from 3 mice per group). Student's *t*-test, ***p<0.001.

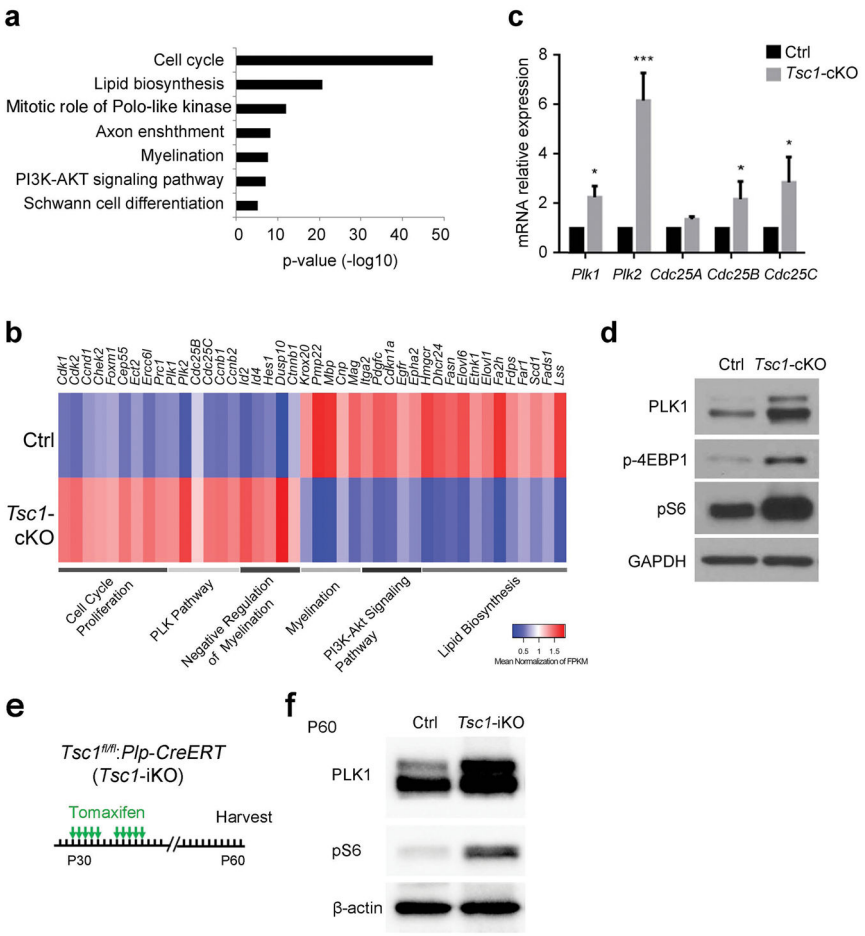

Figure 6. *Tsc1* ablation-induce hypomyelination is dependent on Polo-like kinase signaling

(a) Gene ontology analysis of pathways altered in P7 *Tsc1*-cKO sciatic nerves compared with their control littermates.

(b) Heat map of differentially regulated pathway in *Tsc1*-cKO sciatic nerves compared with control littermates.

(c) qRT-PCR of mRNA expression of PLK pathway genes in control and *Tsc1*-cKO sciatic nerves at P7. n = 3 independent experiments. Student's *t*-test, ***p<0.001, *p<0.05.

(d) Western blot showing expression of PLK1, p-S6, and p-4EBP1 in P7 control and *Tsc1*-cKO sciatic nerves. Blots are representative of triplicate experiments. GAPDH was used as a loading control.

(e) Schema for post-natal knockout of *Tsc1* in Schwann cells

(f) Western blot of PLK1 and pS6 expression at P60 *Tsc1*-iKO mutants and control sciatic nerves after 10 days Tamoxifen injection at P30. β-actin was loaded as a control.

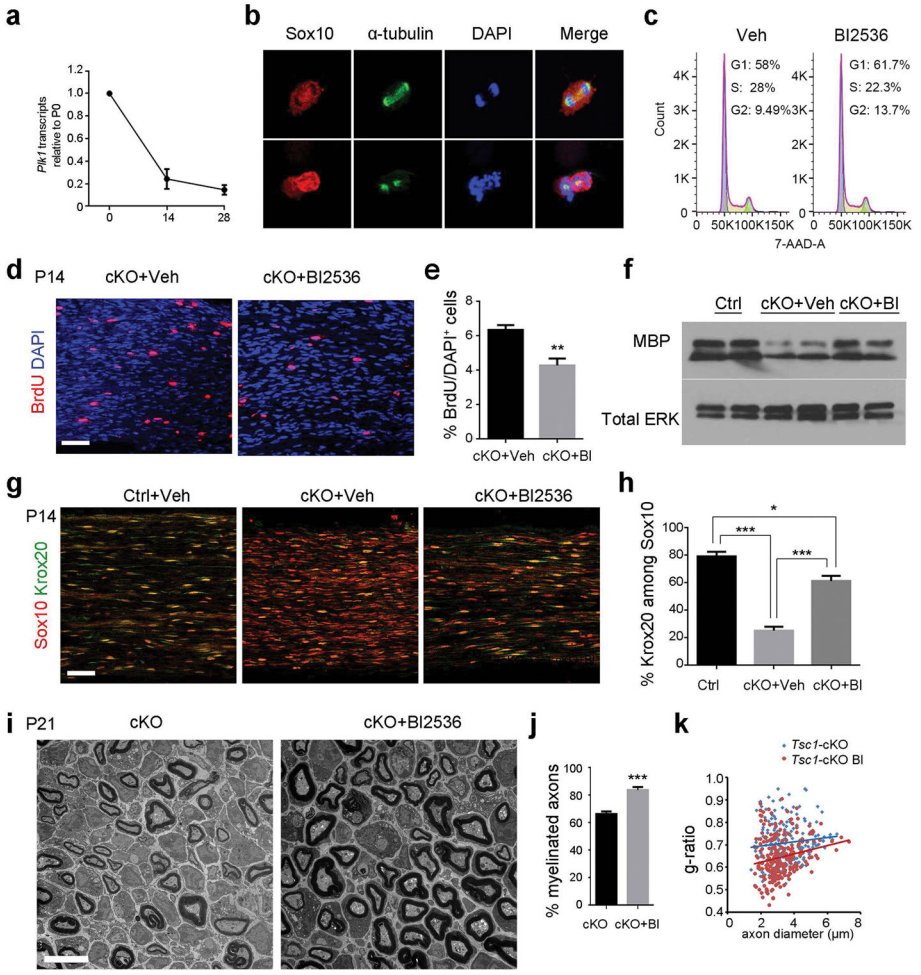

Figure 7. PLK inhibitor treatment partially rescues the hypomyelination defect in the *Tsc1*-cKO mutant

(a) qRT-PCR of mRNA expression of PLK1 in WT sciatic nerves at P0, P14 and P28. n = 3 animals/group.

(b) Representative images of primary rat SCs treated with BI-2536 or vehicle and stained for Sox10, alpha-tubulin, and DAPI. Scale bar, 10 μm.

(c) Representative images showing Cell cycle distributions of DMSO or 100 nM BI-2536 treated Schwann cells.

(d) Representative images showing BrdU staining of P14 *Tsc1*-cKO mutants treated with vehicle or with BI-2536. Scale bar, 50 μm.

(e) Quantification of percentages of $BrdU^+$ cells in *Tsc1*-cKO mutants treated with vehicle or with BI-2536. n = 3 animals/group. Student's *t*-test, ** $p<0.01$.

(f) Western blot showing MBP expression in representative P21 control treated with vehicle and *Tsc1*-cKO mice treated with vehicle or with BI-2536. Total Erk amount as a loading control.

(g)Representative images of P14 control treated with vehicle and *Tsc1*-cKO mutants treated with vehicle or BI-2536. Sciatic nerves were stained with antibodies to Sox10 and Krox20. Scale bar, 50 μm.

(h) Quantification of percentages of Krox20^{+} cells in controls treated with vehicle and *Tsc1*-cKO mutants treated with vehicle or with BI-2536. n = 3 in independent experiments. One way ANOVA with Tukey *t*-test was used to determine significance, *p<0.05, ***p<0.001.
(i) Representative electron micrographs showing ultrastructure of sciatic nerves in *Tsc1*-cKO mutants treated with vehicle or with BI-2536 at P21.
(j) Quantification of percentages of myelinated axons in *Tsc1*-cKO mutants treated with vehicle or with BI-2536 at P21 (n > 200 myelinated axons from 3 animals per group). Student's *t*-test, *** p<0.001.
(k) Quantification of g-ratio in *Tsc1*-cKO mutants treated with vehicle or with BI-2536 at P21 (> 200 axon counts from 3 mice per group).